

Article

# Two- and Three-Stage Natural Gas Combustion System—Experimental Comparative Analysis

Ireneusz Pielecha \*  and Filip Szwajca 

Faculty of Civil and Transport Engineering, Poznan University of Technology, 60-965 Poznan, Poland; filip.szwajca@put.poznan.pl

\* Correspondence: ireneusz.pielecha@put.poznan.pl; Tel.: +48-61-224-4502

**Abstract:** The use of fuels with tendencies to reduce carbon dioxide emissions, particularly gaseous fuels, and improve combustion systems is one of the directions for increasing an internal combustion engine's attractiveness as a power source. This article presents the effects of combining natural gas combustion with a multi-stage combustion system. A two- and three-stage lean charge combustion system was proposed in order to increase the energy system efficiency. In order to achieve this, a single-cylinder test engine was used, with two interchangeably implemented combustion systems. The tests were carried out with two values of the excess air coefficient ( $\lambda = 1.3$  and  $\lambda = 1.5$ ), as well as two different fuel dose values ( $q_0 = 0.35$  and  $0.55$  mg/inj), injected into the prechamber at the same indicated mean effective pressure value (IMEP = 6.5 bar) and the same engine speed ( $n = 1500$  rpm). Based on the obtained research results, it was found that the use of a three-stage system limited the maximum combustion pressure and heat release rate due to the increased resistance of flows between the chambers. At the same time, it was found that the increase in the engine's indicated efficiency took place in a two-stage system, regardless of the excess air coefficient. Changing the dose of fuel fed into the prechamber significantly affects the engine performance (and efficiency) but only in the two-stage combustion system.

**Keywords:** combustion system; TJI system; prechamber; combustion process repeatability; combustion efficiency



**Citation:** Pielecha, I.; Szwajca, F. Two- and Three-Stage Natural Gas Combustion System—Experimental Comparative Analysis. *Energies* **2023**, *16*, 3837. <https://doi.org/10.3390/en16093837>

Academic Editors: Jaroslaw Krzywanski and Wojciech Nowak

Received: 20 March 2023

Revised: 22 April 2023

Accepted: 27 April 2023

Published: 29 April 2023



**Copyright:** © 2023 by the authors. Licensee MDPI, Basel, Switzerland. This article is an open access article distributed under the terms and conditions of the Creative Commons Attribution (CC BY) license (<https://creativecommons.org/licenses/by/4.0/>).

## 1. Introduction

The use of an internal combustion engine as an on-board energy source requires continuous engine design improvement in accordance with the changing emission standards that determine whether the vehicle can be approved for operation. The increasing requirements mainly concern the engine's environmental impact, as well as its impact on human health. Thanks to, among others, improvements in the mixture formation system and the combustion system [1,2], it becomes possible to reduce the harmful exhaust components and the increase in the efficiency of the energy conversion. One of the methods of increasing the feasibility of the modern internal combustion engine as a source of mechanical energy is the lean dose combustion in the cylinders, which allows to increase the efficiency of the system by reducing the heat losses (relationship between specific heat and temperature) and reduce the pumping losses, depending on the engine load. In addition, lower maximum temperatures result in lower exhaust emissions of nitrogen oxides (NO<sub>x</sub>). Diluting the fuel dose also increases the knock resistance, which enables a wider adjustment of the ignition advance angle [3]. Unfortunately, the combustion of lean mixtures is associated with a significant decrease in the operating efficiency of the three-way catalytic converter (TWC), which is widely used in SI engines [4]. However, this problem can be solved by using Lean NO<sub>x</sub> Trap (LNT) [5,6] or selective catalytic reduction (SCR) [7].

As the fuel dose supplied to the cylinder becomes increasingly leaner, the requirements for the minimum ignition energy also increase, the value of which increases with the value

of the excess air coefficient— $\lambda$  [8]. Hence, research is being carried out on ignition systems that generate increasing ignition energy of the main fuel dose: laser ignition (LI), Radio Frequency Based Corona Ignition (RFCI), Microwave-Assisted Spark Ignition (MASI) and Turbulent Jet Ignition (TJI) [9].

By using a combustion system equipped with a prechamber (TJI), with a spark plug (passive prechamber) and, optionally, a fuel supply channel (active prechamber), allows igniting the main charge by funneling burning mixtures through the chamber's holes and not directly from the primary ignition source. Through this method, it is possible to extend the range of the mixture's effective flammability above the value  $\lambda = 1.5$ , in which the conventional system of the SI engine becomes unstable [10,11]. Combustion systems with an ignition chamber are characterized by a greater heat release rate, which is particularly important in the case of fuel–air mixtures with a low laminar flame speed [12,13]. Burkardt et al. conducted research on a single-cylinder SI engine [14] fueled with alcohol with a compression ratio of 16.4, which showed an increase in the maximum value of the excess air coefficient from  $\lambda = 1.7$  for the conventional configuration of the system up to  $\lambda = 2.0$  for the system with an ignition chamber. For the PC configuration, a higher indicated efficiency was achieved, with a maximum value of 46.5% at  $n = 2000$  rpm and an indicated mean effective pressure IMEP = 15 bar.

The two-stage combustion system was characterized by a different structure and control method, which directly affected the engine performance [15]. The simplest solution was to use a prechamber spark plug, which could replace conventional spark plugs without significant interference with the engine design. Comparative studies of conventional plugs with PC plugs of four different geometries [16] indicate an increase in engine operation stability, shortening of the CA<sub>10–90</sub> combustion time and shifting the limit value of the excess air coefficient for stable engine operations. The recorded optical signal indicated a combustion start delay and an increased flame intensity. In addition, a reduction in specific fuel consumption compared to the conventional solution was noted [17]. The disadvantage of the solution, however, was the tendency to create deposits inside the chamber near the electrodes, as well as the lack of additional control of the ignition event. In addition to the passive system based on a prechamber equipped with a spark plug, there are also systems where the ignition chamber is an additional element not permanently connected with the spark plug [13,18].

Another system configuration with a split combustion chamber is a system with an active chamber where an additional dose of fuel is delivered to the vicinity of the primary ignition source, shifting the effective combustion process towards leaner fuel dose ranges [19]. In addition to the fuel dose, air can also be supplied to the chamber for additional flushing, reducing the specific fuel consumption and increasing the share of exhaust gases recirculated by the EGR [20,21]. Due to high thermal loads, depending on the fuel used, systems with a check valve [22] or direct injection (DI) injectors [23] are used. The use of an additional injection system for the PC makes it possible to significantly diversify the fuel dose composition between the working spaces. An example is the co-combustion of hydrogen and methane, where hydrogen is supplied to the chamber, causing a rise in the energy indicators values [24].

The TJI combustion system operation is significantly influenced by the interior geometry of the ignition chamber, as well as the geometry of the outlet openings. This affects the mass transfer and the movement and mixing of the fuel dose around the spark plug. Experimental and simulation studies [25] indicated that the most favorable volume of the ignition chamber is about 5% of the total volume of the main combustion chamber. Positive effects of reducing the outlet hole's diameter with the increase of the excess air coefficient were noted. Using a single-cylinder internal combustion engine operating at  $n = 4500$  rpm under a heavy load, IMEP = 12.5 bar, the effects of using two six-hole chambers (PC1 and PC2) with the volumes/diameters of holes 600/0.7 and 900/0.5 mm<sup>3</sup>/mm were compared in the passive mode [26]. The obtained efficiency was PC1 = 43.4% and PC2 = 43.5% compared to 30.3% for the conventional system. The use of the PC1 chamber turned out to

be better based on energy indicators, while PC2 showed better emission indicators. Optical methods were used to study the effects of radial twisting of the chamber outlet openings by 20 deg at a  $\lambda = 1.3$  methane/air mixture in a rapid compression machine (RCM) [27]. The use of straight holes resulted in higher combustion pressure and a greater heat release rate (HRR). The obtained images indicated a later combustion initiation for the chamber with straight holes and a higher flame intensity 2.52 ms after ignition. Experimental work was also carried out on the impact of splitting the fuel dose between the main and prechambers and variants of the excess air coefficient for six chamber geometries, indicating energy benefits from minimizing the size of the dose for the prechamber PC [28,29].

For further work on the prechamber combustion system, see [30,31], where the authors decided to combine an active combustion system based on a prechamber and a system of direct fuel supply through a one-way valve with a passive prechamber spark plug system. Due to the ecological benefits [30,31], it was decided to conduct the research for natural gas and use the active TJI system, which was tested on a large scale, as a reference point.

## 2. Aim and Scope of Research

The solutions of the two-stage system and its modifications presented above indicate a high efficiency potential for these systems, especially in the case of the lean mixture combustion. This paper presents a direct comparison of both combustion systems. Since the work was carried out on the same test setup, it was possible to analyze the same values under the same conditions.

Two queries about the thermodynamics of the process were stated: (1) how the excess air coefficient affects the combustion process and (2) how the fuel dose fed into the prechamber affects the combustion process. These two questions, in connection with the two combustion systems, made it possible to indicate which system was characterized by a greater efficiency in the specific test conditions. The fundamental difference between the systems mainly comes down to the different inter-chamber throttling between the cylinder volume and the ignition electrodes and, in the case of a three-stage system, feeding an additional dose of fuel between the smaller chambers.

## 3. Materials and Methods

### 3.1. Test Stand

The tests of the combustion systems were carried out on the single-cylinder research engine AVL 5804 with the eddy current brake AVL AMK DW13-170. The engine was adapted for the combustion of gaseous fuels and was equipped with an ignition system. The cylinder head was adapted to the two- and three-stage systems. An active prechamber (with gaseous fuel supply) was used. Engine specifications are provided in Table 1.

**Table 1.** Technical data of the single-cylinder test engine used.

| Parameter         | Unit            | Value                            |
|-------------------|-----------------|----------------------------------|
| Engine            | –               | 1-cyl., 4-valve, SI, TJI         |
| Displacement      | dm <sup>3</sup> | 0.5107                           |
| Bore × stroke     | mm              | 85 × 90                          |
| Compression ratio | –               | 15.5                             |
| Fueling           | –               | DI and PFI (EM injectors); 7 bar |
| Prechamber        | –               | 2-stage (spark plug M10)         |
| Air system        | –               | 3-stage (spark plug M12)         |
|                   |                 | Naturally aspirated              |

The diagram of the test stand and the parameters it measured are shown in Figure 1. The mass flow rate of fuel and air, as well as the thermodynamic parameters of the intake air, exhaust gases and gaseous fuel, were all controlled. The temperature of the cooling liquid and lubricating oil was constant at 70 °C.

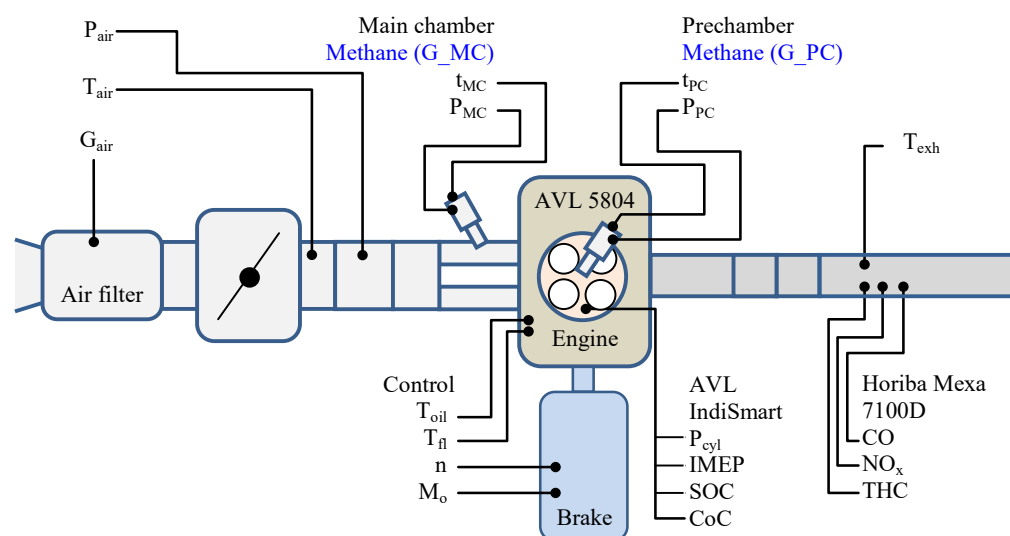


**Figure 1.** Schematic of the test stand for 2- and 3-stage combustion systems.

The combustion systems' tests included using a 2-stage system (Figure 2a) and a 3-stage system (Figure 2b). For both cases, the same prechamber was used, which parameters are presented in Table 2. Both tested systems used an active combustion chamber, which means that fuel was injected into the prechamber and ignited. In each case, only fuel without air was supplied to the prechamber. The spark plug had its own chamber that the mixture formed in the prechamber was fed into for the three-stage system (Figure 2b). In the two-stage system, the chamber had a volume of  $1.8 \text{ cm}^3$  and 7 outlet holes with a diameter of  $1.5 \text{ mm}$ . In the three-stage system, the volume of the prechambers was  $2.55 \text{ cm}^3$  and the PC spark plug had six holes with a diameter of  $1 \text{ mm}$ . In the 2-stage system, the volume of the ignition chamber was  $5.19\%$  of the volume of the combustion chamber (piston at the TDC); in the three-stage system, this share was larger and reached about  $7.35\%$ .

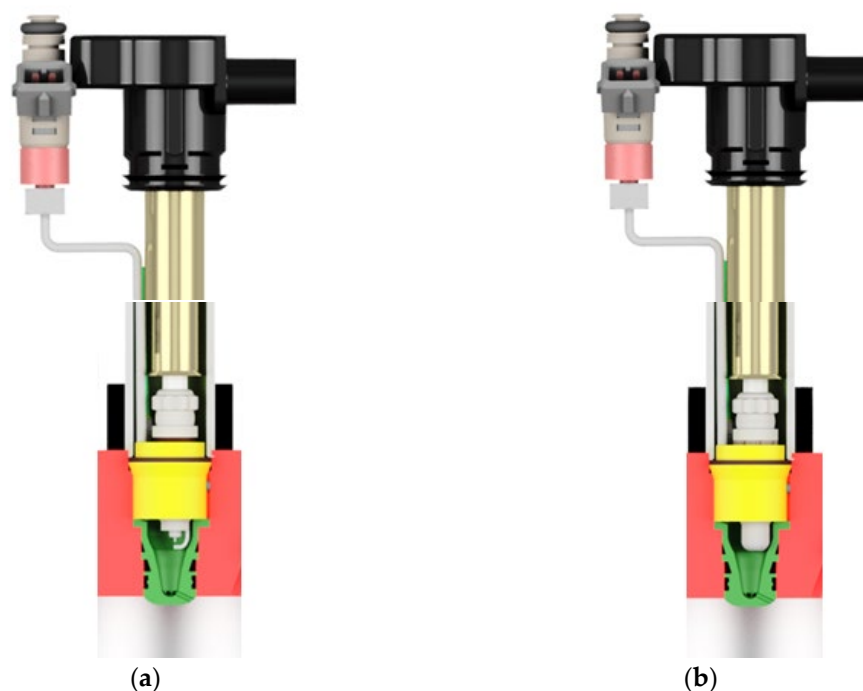


**Figure 2.** Picture of the combustion systems: (a) two-stage system with an active prechamber and (b) three-stage system with an active prechamber and its own spark plug chamber.

**Table 2.** Technical specifications of the prechamber used in the research.

| Parameter       | Unit            | Value |
|-----------------|-----------------|-------|
| Number of holes | –               | 7     |
| Hole diameter   | mm              | 1.5   |
| Volume          | cm <sup>3</sup> | 1.8   |
| Spark plug      |                 | M10   |

Combustion thermodynamic studies were carried out using the AVL GH14D (main chamber) and Kistler 6081 (prechamber) combustion pressure sensors and a Horiba Mexa 7100D combustion analyzer. Data recording was performed at a high data acquisition rate using the AVL IndiSmart system with AVL IFEM charge amplifiers. Methane consumption in the prechamber (qo\_PC) and main chamber (qo\_MC) was measured using mass flow meters. Technical specifications of the measuring equipment used in the tests are given (Table 3).

**Table 3.** Technical data of the test equipment.

| Parameter              | Type                               | Range                                                                    |
|------------------------|------------------------------------|--------------------------------------------------------------------------|
| Fast-varying processes | AVL IndiSmart                      | 8-channel + amplifiers IFEM                                              |
| Pressure sensor MC     | AVL GH14D                          | 0–250 bar                                                                |
| Pressure sensor PC     | Kistler 6081 AQ22                  | 0–250 bar                                                                |
| Air-flow meter         | ABB SensyFlow                      | 0–720 kg/h; error < ±0.8%                                                |
| Fuel-flow meter MC     | Micro Motion ELITE CMFS010M        | 0.1–2 kg/h; accuracy ±0.25%                                              |
| Fuel-flow meter PC     | Bronkhorst 111B                    | 0.1–100 g/h; accuracy ±0.5%<br>RD plus ±0.1% FS                          |
| Crank angle            | AVL 365C                           | 0.1 deg                                                                  |
| Lambda-value           | Bosch LSU4.9                       | λ~10                                                                     |
| Injection time PC/MC   | Custom design<br>Horiba Mexa 7100D | t <sub>inj</sub> = 0–20 ms; α = var                                      |
| Exhaust analyzer       | NDIR<br>FID<br>CLD                 | CO(L)—50–5000 ppm<br>THC—10–50,000 ppm<br>NO <sub>x</sub> —10–10,000 ppm |

### 3.2. Test Conditions

The tests observing the in-cylinder processes and measuring the exhaust emissions for the two different combustion systems were carried out at a constant engine speed  $n = 1500$  rpm and at IMEP = 6.5 bar and for two values of the excess air coefficient. The engine operation stability criterion was defined as the engine operation non-repeatability determined by the value of the CoV(IMEP) coefficient < 3.0% [32] (older sources assigned this indicator a value of 10% [33]; sometimes, intervals were defined to obtain stable or semi-stable combustions [32]). This indicator was defined as:

$$\text{CoV(IMEP)} = 100 \times \frac{\sigma(\text{IMEP})}{\mu(\text{IMEP})}, \quad (1)$$

where  $\sigma$  and  $\mu$  are the standard deviation and the mean value, respectively, over a number of consecutive combustion cycles (the analysis includes 100 cycles).

To determine the heat release, a model was used that takes into account changes in the pressure and volume in the cylinder:

$$\frac{dQ_{\text{net}}(\alpha)}{d\alpha} = \frac{\gamma}{\gamma - 1} P(\alpha) \frac{dV(\alpha)}{d\alpha} + \frac{1}{\gamma - 1} V(\alpha) \frac{dP(\alpha)}{d\alpha}, \quad (2)$$

where  $P$  is the instantaneous cylinder pressure,  $\alpha$  is the crank angle,  $\gamma$  is the ratio of the specific heats and  $V$  is the instantaneous cylinder volume.

During the tests, the assumption was made that the ignition angle will be the control value, to be adjusted to achieve a constant CoC value:

$$\alpha_{ia} = f(\text{IMEP}, q_{o\_PC}, \lambda) = \text{var} \rightarrow \text{CoC} = \text{const.} \quad (3)$$

The CoC value was defined as the crankshaft angle, at which 50% of the heat had been released:

$$\text{CoC} = \alpha \text{ at } 0.5 \times \int_{\text{SOC}}^{\text{EOC}} \frac{dQ_{\text{net}}}{d\alpha} d\alpha, \quad (4)$$

where SOC—start of combustion and EOC—end of combustion. The start of combustion (the angle at which 5% of the heat was released) and the end of combustion (the angle at which 90% of the heat was released) were determined in a similar way.

The combustion process (i.e., the ignition angle) was controlled in such a way as to maintain constant values of the combustion center (CoC = 8 deg aTDC).

The maximum indicated engine efficiency was determined using the following equation:

$$\eta_i = \frac{1}{g_i \times L_{\text{HV}}}, \quad (5)$$

where LHV—methane calorific value and  $g_i$ —indicated specific fuel consumption:

$$g_i = \frac{G_{\text{MC}} + G_{\text{PC}}}{N_i}, \quad (6)$$

where  $G$ —fuel mass consumption, respectively, in the main chamber (MC) and prechamber (PC) and  $N_i$ —indicated power, expressed by the equation:

$$N_i = \frac{V_s \times \text{IMEP} \times n}{\tau}, \quad (7)$$

where  $V_s$ —engine displacement,  $n$ —rotational speed and  $\tau$ —the cyclical nature of engine operations.

For a known engine power, the values of specific exhaust emissions of carbon monoxide (CO), total emissions of hydrocarbons (THC) and nitrogen oxides (NO<sub>x</sub>) were also calculated.

With the set test conditions and control strategies for the combustion process (Table 4), tests were carried out by registering 100 consecutive cycles of engine operation.

**Table 4.** Research method specifications.

| Combustion System | Test Conditions                                                                                                                                                           | Control Strategy                                                       |
|-------------------|---------------------------------------------------------------------------------------------------------------------------------------------------------------------------|------------------------------------------------------------------------|
| 2-stage           | $n = 1500 \text{ rpm}$<br>$\text{IMEP} = 6.5 \text{ bar}$                                                                                                                 | $\text{CoC} = 8 \text{ deg aTDC}$<br>$\text{CoV}(\text{IMEP}) < 3.5\%$ |
| 3-stage           | $\lambda = \sim 1.3; \sim 1.5$<br>$q_{o\_PC} = \begin{cases} \text{small} & \sim 0.35 \text{ mg/inj} \\ \text{large} & \sim 0.55\text{--}0.60 \text{ mg/inj} \end{cases}$ | $q_{o\_PC} + q_{o\_MC} = \text{const.}$                                |

An example characteristic of the measured fast-varying values recorded during the tests is shown in Figure 3. Fuel was injected into both combustion chambers at a pressure of 7 bar and at a constant value of the angle  $\alpha = 300 \text{ deg bTDC}$ . As the figure shows, the injection time of the prechamber fuel dose was significantly shorter than the fuel injection time into the main chamber. Additionally, a flange was used between the injector and the return valve.

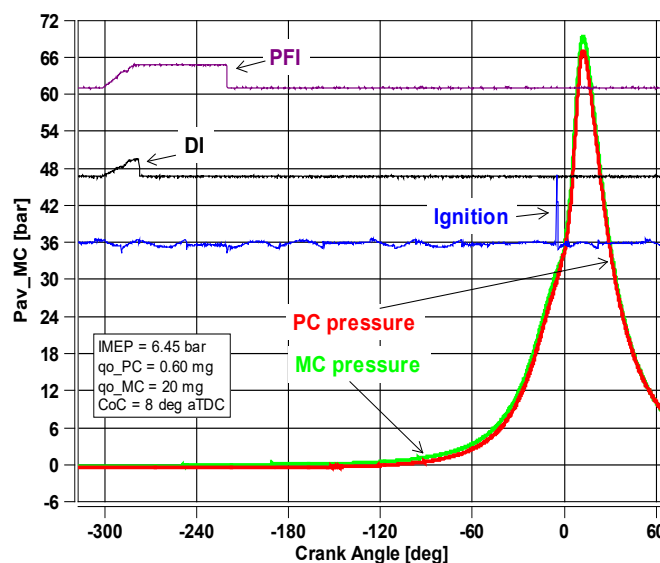


**Figure 3.** An example characteristic of variable signals with an indication of the gas supply conditions to the prechamber and to the main chamber.

According to Equation (1), the non-repeatability of the engine operation was determined by using data from 100 successive engine operation cycles. The data in Table 5 indicate acceptable engine operating conditions. The CoV(IMEP) did not exceed 1.11%, which indicated stable engine operations under all test conditions.

**Table 5.** Engine operation non-repeatability values CoV(IMEP) calculated using Equation (1).

| Combustion System | $\lambda$ | qo_PC → Small | qo_PC → Large |
|-------------------|-----------|---------------|---------------|
| 2-stage           | 1.3       | 1.02          | 1.08          |
|                   | 1.5       | 1.02          | 0.88          |
| 3-stage           | 1.3       | 1.11          | 1.10          |
|                   | 1.5       | 1.10          | 1.08          |

#### 4. Thermodynamic Analysis of the Combustion Systems

##### 4.1. Size of Initial and Main Fuel Dose Used in the Conducted Tests

In the tests, the fuel dose fed into the prechamber was adjusted, along with the main dose for the main chamber (Figure 4). This was to keep the total fuel dose constant. The value of the excess air coefficient changed to a certain extent, which was caused by using a one-cylinder engine (despite the use of an additional air compensating tank). Changes in the injected fuel dose were done by controlling the injection time and not from directly changing the fuel dose itself. At the same time, the change in the excess air coefficient caused a change in the intake manifold pressure, which also affects the value of the fuel dose mass.

The combustion process analysis was carried out by first comparing the pressure changes for both systems at different values of  $\lambda$ . The three-stage system (Figure 5) was characterized by an increase in the resistance of the inter-chamber flows, which resulted in lower pressure values, regardless of the tests conditions. A small dose of fuel fed into the prechamber resulted in a combustion process improvement, as the maximum pressure in the main chamber (Pmx) was higher (by 3.7%) than when a large fuel dose was fed into the PC. Increasing the excess air ratio did not significantly change the Pmx; the changes were below 0.5% (with the same combustion system).

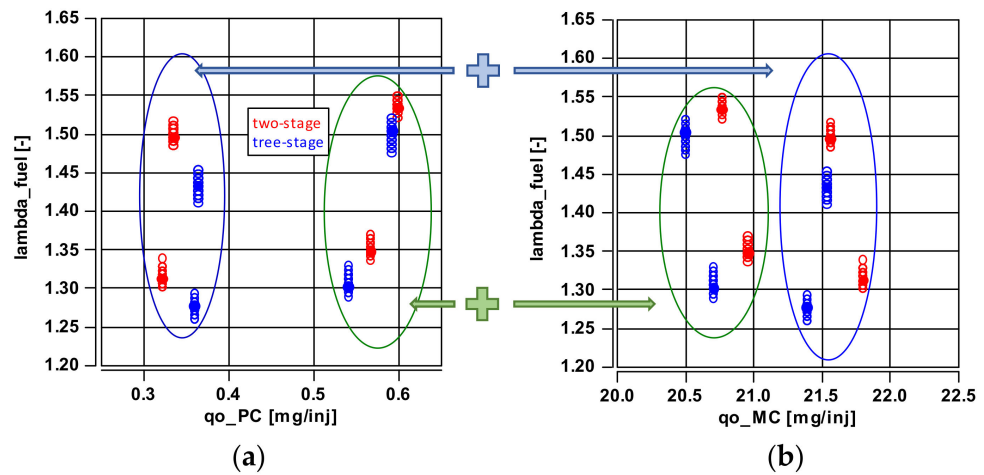


**Figure 4.** Conditions when conducting multi-stage combustion engine systems tests: (a) the initial dose size fed into the prechamber ( $qo_{PC}$ ) at different values of the excess air coefficient and (b) the main chamber ( $qo_{MC}$ ); during combustion, the value of the sum of the fuel doses was kept constant in accordance with the control strategy (Table 4).

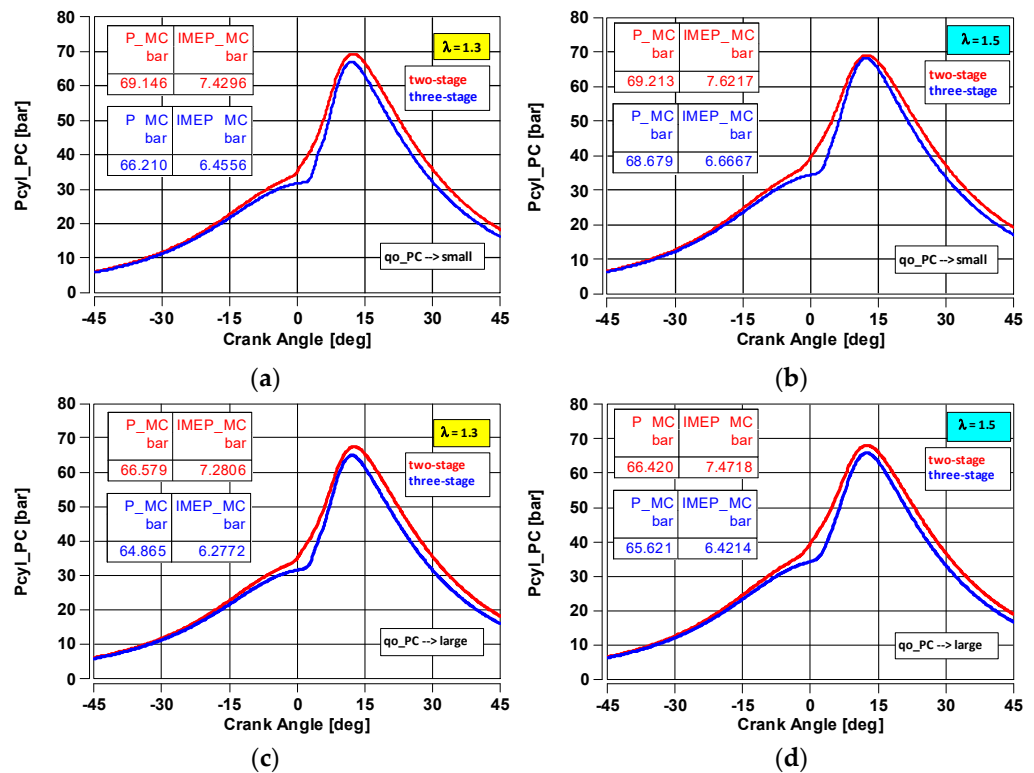


**Figure 5.** The cylinder combustion pressure characteristic (in the main chamber) for both combustion systems: (a) for the small initial dose value ( $qo_{PC} = \sim 0.35$  mg/inj) and  $\lambda = 1.3$ , (b) for the small initial dose value ( $qo_{PC} = \sim 0.35$  mg/inj) and  $\lambda = 1.5$ , (c) for the large initial dose value ( $qo_{PC} = \sim 0.6$  mg/inj) and  $\lambda = 1.3$  and (d) for the large initial dose value ( $qo_{PC} = \sim 0.6$  mg/inj) and  $\lambda = 1.5$ .

Comparative analyses of the combustion systems indicated a more favorable Pmx curve in the two-stage system (4% increase), regardless of the size of the dose fed into the prechamber. Increasing the excess air coefficient to  $\lambda = 1.5$  reduced the differences between the peak pressure Pmx values (maximum change observed was 1.5%).

The IMEP value caused more significant differences between the combustion systems. At  $\lambda = 1.3$  (regardless of the  $q_{o\_PC}$  dose), the change was over 12% (in favor of the two-stage system). Changing the engine operating conditions at  $\lambda = 1.5$  resulted in the same IMEP changes in favor of the two-stage system.

The analysis of the rate of the combustion pressure changes indicated clear two-stage changes in the pressure build-up in the two-stage system. Burning a small dose in the prechamber resulted in a large value of the maximum pressure increase. During three-stage combustion, it was not possible to visually isolate each of the combustion phases from the obtained data. Nevertheless, the pressure increased more. This means that the initial combustion process was more dynamic. It should be noted that there is a significant delay (about 4 deg) in the start of the combustion process in the three-stage system. This was not a result of the fuel dose preparation conditions being worse but only from the need to maintain the selected combustion strategy (CoC = 8 deg aTDC). This means that the increased dynamics of the combustion process allowed the ignition to be delayed by about 3 deg compared to the two-stage combustion system.

A large dose of  $q_o$  injected into the PC resulted in more steady pressure changes (in the three-stage system). There was still a delay in the rate of the pressure changes (only by about 3 deg CA) compared to the two-stage system. At  $\lambda = 1.5$  and a large  $q_{o\_PC}$  dose value, a reduction in the cylinder pressure changes was observed in both systems.

The delayed start of the combustion process, notable in Figure 6, also had an impact on the heat release. The values of the net heat release rate (ignoring heat losses to the walls) were determined based on Equation (2)—see Figure 7. The maximum heat release rate observed in the two-stage system at a small fuel dose ( $q_{o\_PC}$ ) was lower by about 10–12% compared to a larger dose. At  $\lambda = 1.5$ , the changes were even greater and amounted to 10–17% in favor of the three-stage system and a small fuel dose ( $q_{o\_PC}$ ). Not only was the  $dQ_{mx}$  greater but the slope of the curves in the three-stage system was also greater (both during the build-up and limiting the heat release). This indicated a more rapid process, which was also confirmed by the analysis of the cylinder pressure and the rate of the pressure change.

The maximum heat release rates were higher in the three-stage combustion system, irrespective of the values of the fuel dose ( $q_{o\_PC}$ ) and  $\lambda$ . At the same time, the angle range of the  $dQ_{MC}$  changes was smaller than in the case of the two-stage combustion system. This indicates that such a system can be used in engines with higher rotational speeds.

The integral heat release rate was calculated to obtain information about the overall combustion process. Through such calculations, it was possible to determine the combustion process quality of the multi-stage combustion systems (Figure 7). The three-stage system was characterized by lower values of the total heat released ( $Q_{mx}$ ) by about 9–14% compared to the two-stage system (regardless of the  $q_{o\_PC}$  and  $\lambda$ ). Within the same combustion system, increasing the  $q_{o\_PC}$  resulted in only a 3% change in the  $Q_{mx}$  values. Increasing the value of  $\lambda$  improved the obtained heat release values but only in the case of the three-stage combustion system, which may indicate the importance of using even leaner mixtures in the three-stage system.

Analyzing the thermodynamic indicators (Figure 8) pointed towards the two-stage system having a greater potential, at least in terms of the analyzed quantities ( $0.35 \text{ mg/inj} < q_{o\_PC} < 0.60 \text{ mg/inj}$  and  $1.3 < \lambda < 1.5$ ). However, the three-stage system has shown great results in terms of the fuel combustion rate: large values of the pressure increase and an overall shorter combustion process. The above thermodynamic quantities, in terms of intra-cylinder processes, were supplemented with engine operation indicators in the next section.

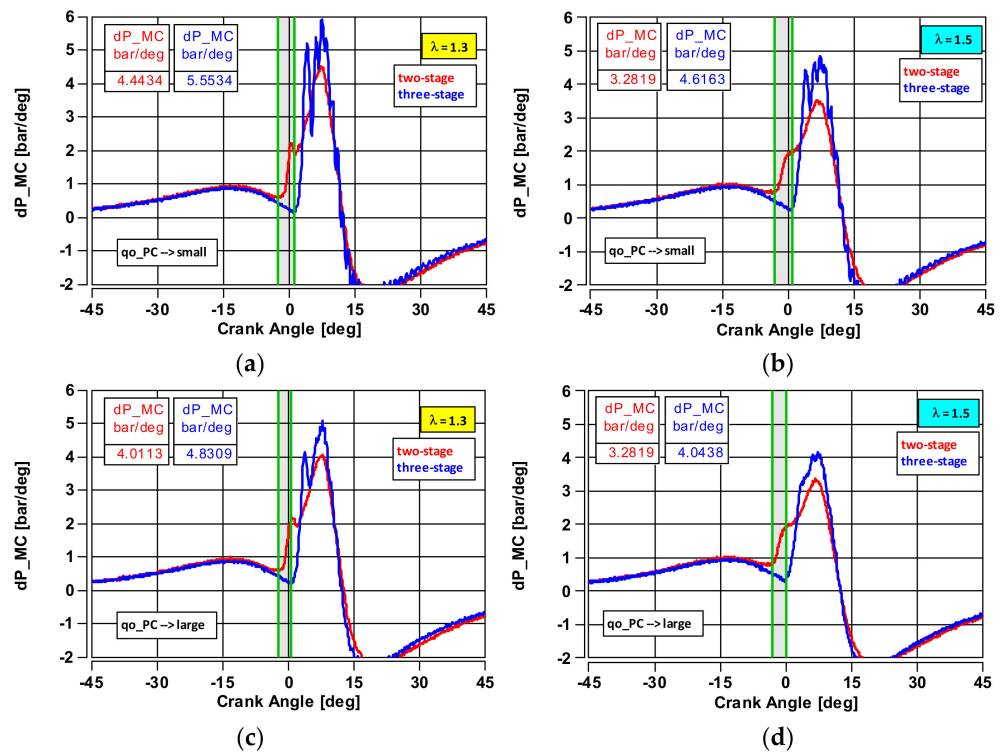


**Figure 6.** The combustion pressure increase rate in the cylinder (in the main chamber) for both combustion systems: (a) for a small initial dose value ( $q_{o\_PC} = \sim 0.35$  mg/inj) and  $\lambda = 1.3$ , (b) for a small initial dose value ( $q_{o\_PC} = \sim 0.35$  mg/inj) and  $\lambda = 1.5$ , (c) for a large initial dose value ( $q_{o\_PC} = \sim 0.6$  mg/inj) and  $\lambda = 1.3$  and (d) for a large initial dose value ( $q_{o\_PC} = \sim 0.6$  mg/inj) and  $\lambda = 1.5$ .

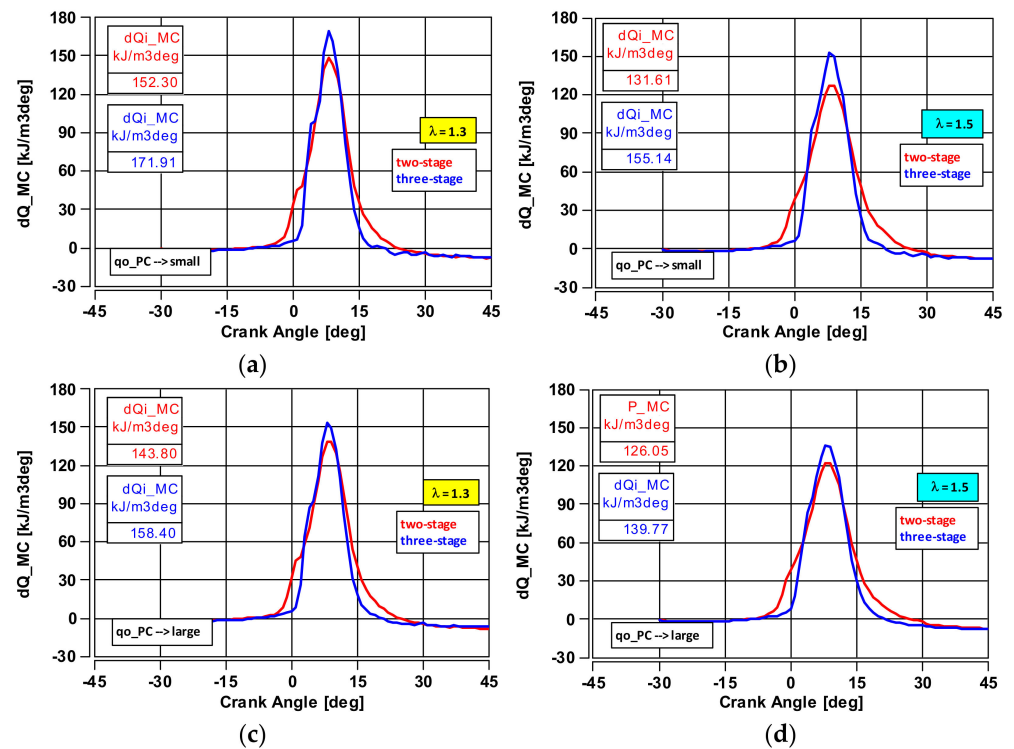


**Figure 7.** The characteristics of the heat release rate in the cylinder (in the main chamber) for both combustion systems: (a) for a small initial dose value ( $q_{o\_PC} = \sim 0.35$  mg/inj) and  $\lambda = 1.3$ , (b) for a small initial dose value ( $q_{o\_PC} = \sim 0.35$  mg/inj) and  $\lambda = 1.5$ , (c) for a large initial dose value ( $q_{o\_PC} = \sim 0.6$  mg/inj) and  $\lambda = 1.3$  and (d) for a large initial dose value ( $q_{o\_PC} = \sim 0.6$  mg/inj) and  $\lambda = 1.5$ .

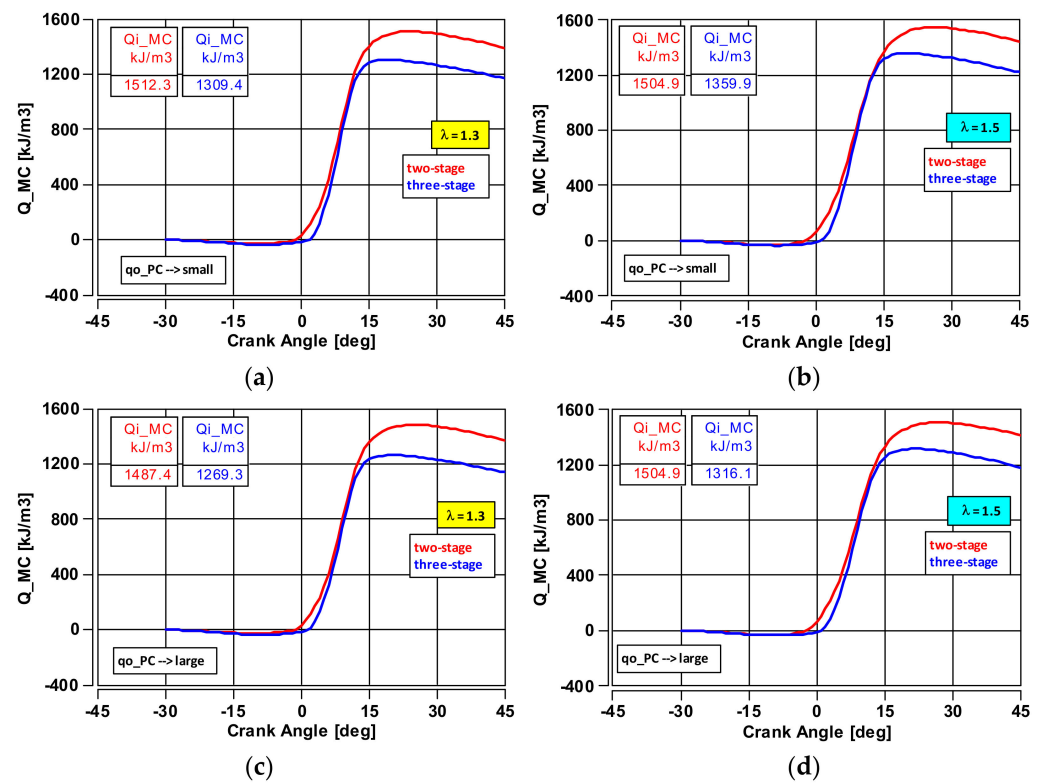


**Figure 8.** The characteristics of the total heat released in the cylinder (in the main chamber) for both combustion systems: (a) for a small initial dose value ( $q_{o\_PC} = \sim 0.35$  mg/inj) and  $\lambda = 1.3$ , (b) for a small initial dose value ( $q_{o\_PC} = \sim 0.35$  mg/inj) and  $\lambda = 1.5$ , (c) for a large initial dose value ( $q_{o\_PC} = \sim 0.6$  mg/inj) and  $\lambda = 1.3$  and (d) for a large initial dose value ( $q_{o\_PC} = \sim 0.6$  mg/inj) and  $\lambda = 1.5$ .

## 4.2. Engine Operation Indicators

### 4.2.1. Thermodynamic Indicators

The measured values were summarized based on the conducted analyses (Figure 9), where the values of the start of combustion (AI05), the combustion center (CoC) and the end of combustion (AI90) were shown. These values were determined as described in Equation (4).

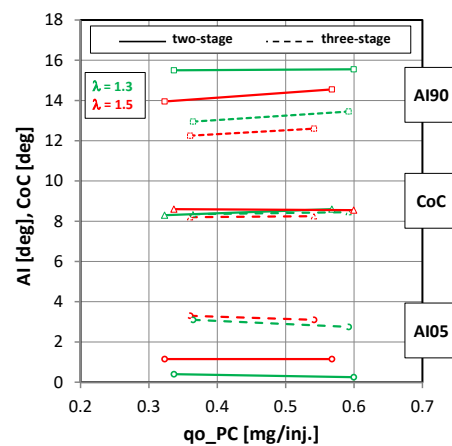


**Figure 9.** Thermodynamic analysis of the combustion process: start of combustion (AI05), center of combustion (CoC) and end of combustion (AI90).

Data analysis showed that, in order to obtain a constant CoC value (8 deg aTDC), the ignition advance needed to be increased in the two-stage system (or reduced in the three-stage system). In the three-stage system, the change of  $\lambda$  (from 1.3 to 1.5) had no effect on the start of combustion. However, increasing  $\lambda$  to 1.5 made it possible to significantly reduce the duration of the entire process (AI(90)–AI(05)).

Based on the previously discussed observations, it was found that multi-stage systems can be dedicated to the combustion of lean mixtures, and in this research, the three-stage system has shown greater potential (with an even higher excess air coefficient than presented in this study).

#### 4.2.2. Fuel Consumption and System Efficiency

The engine operation indicators were determined using Equations (5)–(7). These indicators were the specific indicated fuel consumption (Figure 10a) and engine efficiency (Figure 10b). With the analyzed values of  $\lambda$  (1.3 and 1.5), a much more favorable specific fuel consumption value was observed in the two-stage system (12–14%, irrespective of the excess air coefficient value). Changing the prechamber fuel dose did not affect the specific fuel consumption. This was primarily due to the fact that the total value of the fuel dose was controlled and kept constant during the tests.

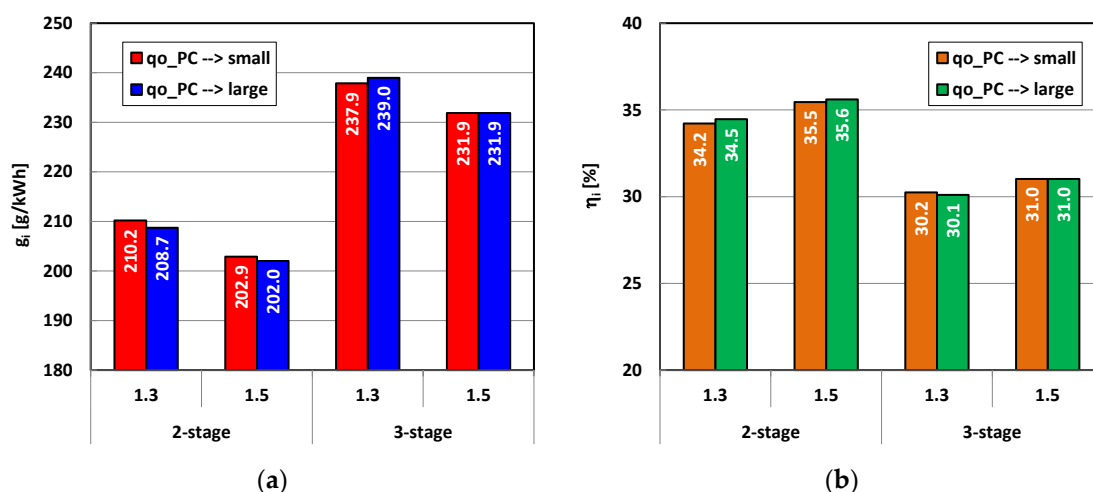


**Figure 10.** Analysis of the engine performance indicators using two combustion systems: (a) specific indicated fuel consumption and (b) indicated engine efficiency.

The indicated engine efficiency obtained for the analyzed combustion systems corresponded with the values of the specific fuel consumption. The mentioned parameters were considered representative energy indicators for comparing combustion systems. Better results were found for the two-stage system (values of about 34.2–35.6%), irrespective of the used excess air coefficient value. A comparison of the combustion systems showed a significant improvement in the efficiency, reaching 13–14% when using the two-stage system.

The exhaust emission analysis was carried using the recorded data of each exhaust gas component's concentrations. The Horiba Mexa 7100D analyzer used for the research allowed the measurement of the total hydrocarbons (non-methane hydrocarbons were not analyzed). Taking into account the mass of the exhaust gas (calculated using the fuel consumption and air flow), as well as the density coefficients of the exhaust gas components ( $i_{CO} = 0.000966$ ,  $i_{THC} = 0.000479$  and  $i_{NOx} = 0.001587$ ) [34], the engine power ( $N_i$ ) was used to calculate the power-specific exhaust emission of each exhaust component. The emissions shown are raw emissions without the use of an aftertreatment system.

Hydrocarbon emissions increased with increasing the excess air coefficient value, regardless of the fuel dose injected into the prechamber or the combustion system used

(Figure 11a). This tendency was consistent with previous research [33], and it is caused by excess air and limited flame continuity. There were no large differences in the THC emissions when changing the combustion system from two- to three-stage combustion (an increase of about 5% or 10% at  $\lambda = 1.3$  and  $\lambda = 1.5$ , respectively). In terms of CO emissions, the two-stage system was more advantageous, because, regardless of the value of  $\lambda$ , the exhaust emission values were found to be about 40% lower (Figure 11b). The size of the dose injected into the prechamber in the two-stage system had no effect on the measured exhaust emission values.

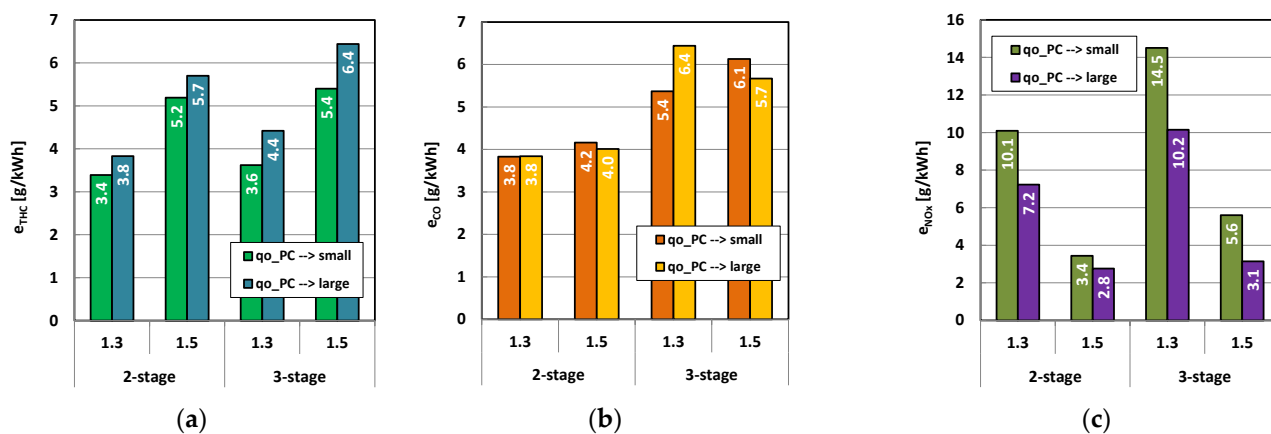


**Figure 11.** Exhaust emission values measured from the multi-stage combustion systems for two different fuel doses fed into the prechamber and for two different values of  $\lambda = 1.3$  and  $\lambda = 1.5$ : (a) hydrocarbons, (b) carbon monoxide and (c) nitrogen oxides.

Multi-stage combustion systems were found to have a significant effect on the exhaust emission of nitrogen oxides (Figure 11c). The effect of both the initial dose and the  $\lambda$  value became clear in this example. Combustion in the two-stage system resulted in about 30% lower exhaust emission values, irrespective of the  $\lambda$  value. The effect of  $\lambda$  itself was significant in both systems: its increase from  $\lambda = 1.3$  to  $\lambda = 1.5$  resulted in emission reductions by 61–69% in both combustion systems used.

## 5. Conclusions

The experimental results presented in the article show the effect of using an additional combustion chamber integrated with a spark plug, creating, together with the two-stage system, a new concept of three-stage combustion. As a result of comparing the effects of using the two-stage and three-stage combustion systems, significant differences were found, especially in the combustion rate and heat release. Testing the engine for a medium load and engine speed of 1500 rpm, the following advantages of the two-stage system were found:

1. higher maximum combustion pressure in the main chamber (by about 4%);
2. the values of the indicated mean effective pressure (IMEP) were greater by about 12% for the same fuel dose;
3. amounts of the heat released values ( $Q_{mx}$ ) were greater by about 9–14%;
4. higher indicated efficiency, irrespective of the excess air coefficient value (by more than 10%);
5. increasing the fuel dose fed into the prechamber slightly increased the efficiency of the system, irrespective of the excess air coefficient;
6. lower HC emissions (by about 5–10%), lower CO emissions (by about 40%) and lower  $NO_x$  emissions (by about 30%).

The three-stage combustion system, on the other hand, showed potential in:

1. the combustion rates: the increases in the cylinder pressure changes were more rapid, indicating the possibility of rapid combustion of the created mixture; this is particularly important in relation to the combustion of very lean mixtures when the rate drops sharply in conventional systems;
2. limiting the ignition advance angle; this limitation was due to the combustion rate, which allowed the use of higher compression ratios without causing a rise in the engine knock.

**Author Contributions:** Conceptualization, I.P. and F.S.; methodology, I.P. and F.S.; software, I.P. and F.S.; validation, I.P. and F.S.; formal analysis, I.P. and F.S.; investigation, I.P. and F.S.; resources, I.P. and F.S.; data curation, I.P. and F.S.; writing—original draft preparation, I.P. and F.S.; writing—review and editing, I.P. and F.S.; visualization, I.P. and F.S.; supervision, I.P. and F.S.; project administration, I.P. and F.S. and funding acquisition, I.P. and F.S. All authors have read and agreed to the published version of the manuscript.

**Funding:** This research received no external funding.

**Data Availability Statement:** Not applicable.

**Conflicts of Interest:** The authors declare no conflict of interest.

## References

1. Nakata, K.; Nogawa, S.; Takahashi, D.; Yoshihara, Y.; Komagai, A.; Suzuki, T. Engine technologies for achieving 45% thermal efficiency of S.I. Engine. *SAE Int. J. Engines* **2016**, *9*, 179–192. [[CrossRef](#)]
2. Singh, A.P.; Agarwal, A.K. *Novel Internal Combustion Engine Technologies for Performance Improvement and Emission Reduction*; Springer Nature: Singapore, 2022.
3. Hlaing, P.; Echeverri Marquez, M.; Bhavani Shankar, V.S.; Johansson, B.; Cenker, E. A study of lean burn pre-chamber concept in a heavy duty engine. In *SAE Technical*; SAE International: Warrendale, PA, USA, 2019. [[CrossRef](#)]
4. Atis, C.; Schock, H. Comparison of excess air (lean) vs. EGR diluted operation in a pre-chamber air/fuel scavenged dual mode, turbulent jet ignition engine at high dilution rate (~40%). *SAE Int. J. Adv. Curr. Pract. Mobil.* **2021**, *3*, 1569–1584. [[CrossRef](#)]
5. Parks, J.E.; Prikhodko, V.; Partridge, W.; Choi, J.-S.; Norman, K.; Huff, S.; Chambon, P. Lean gasoline engine reductant chemistry during lean NOx Trap Regeneration. *SAE Int. J. Fuels Lubr.* **2010**, *3*, 956–962. [[CrossRef](#)]
6. Murata, Y.; Morita, T.; Wada, K.; Ohno, H. NOx trap three-way catalyst (N-TWC) concept: TWC with NOx adsorption properties at low temperatures for cold-start emission control. *SAE Int. J. Fuels Lubr.* **2015**, *8*, 454–459. [[CrossRef](#)]
7. Prikhodko, V.; Parks, J.; Pihl, J.; Toops, T. Ammonia generation and utilization in a passive SCR (TWC+SCR) system on lean gasoline engine. *SAE Int. J. Engines* **2016**, *9*, 1289–1295. [[CrossRef](#)]
8. Moorhouse, J.; Williams, A.; Maddison, T.E. An investigation of the minimum ignition energies of some C1 to C7 hydrocarbons. *Combust Flame* **1974**, *23*, 203–213. [[CrossRef](#)]
9. Vedharaj, S. Advanced ignition system to extend the lean limit operation of spark-ignited (SI) engines—A review. In *Alternative Fuels and Advanced Combustion Techniques as Sustainable Solutions for Internal Combustion Engines*; Springer: Singapore, 2021; pp. 217–255. [[CrossRef](#)]
10. Stadler, A.; Wessoly, M.; Blochum, S.; Härtl, M.; Wachtmeister, G. Gasoline fueled pre-chamber ignition system for a light-duty passenger car engine with extended lean limit. *SAE Int. J. Engines* **2019**, *12*, 323–339. [[CrossRef](#)]
11. Bunce, M.; Blaxill, H. Methodology for combustion analysis of a spark ignition engine incorporating a pre-chamber combustor. In *SAE Technical*; SAE International: Warrendale, PA, USA, 2014. [[CrossRef](#)]
12. Syrovatka, Z.; Vitek, O.; Vavra, J.; Takats, M. Scavenged pre-chamber volume effect on gas engine performance and emissions. In *SAE Technical*; SAE International: Warrendale, PA, USA, 2019. [[CrossRef](#)]
13. Duan, W.; Huang, Z.; Chen, H.; Tang, P.; Wang, L.; Chen, W. Effects of passive pre-chamber jet ignition on combustion and emission at gasoline engine. *Adv. Mech. Eng.* **2021**, *13*, 1–10. [[CrossRef](#)]
14. Burkardt, P.; Wouters, C.; Pischinger, S. Evaluation of pre-chamber orifice orientation in an ethanol-fueled spark-ignition engine for passenger car applications. *SAE Int. J. Engines* **2022**, *15*, 471–482. [[CrossRef](#)]
15. Alvarez, C.E.; Couto, G.E.; Roso, V.R.; Thiriet, A.B.; Valle, R.M. A review of prechamber ignition systems as lean combustion technology for SI engines. *Appl. Therm. Eng.* **2018**, *128*, 107–120. [[CrossRef](#)]
16. Yamanaka, K.; Shiraga, Y.; Nakai, S. Development of pre-chamber sparkplug for gas engine. In *SAE Technical*; SAE International: Warrendale, PA, USA, 2011. [[CrossRef](#)]
17. Sens, M.; Binder, E. Pre-chamber ignition as a key technology for future powertrain fleets. *MTZ Worldw.* **2019**, *80*, 44–51. [[CrossRef](#)]
18. Maserati Presents Nettuno: The New 100% Maserati Engine that Adopts F1 Technology for a Road Car. Available online: <https://www.maserati.com/gh/en/news/nettuno-engine-mc20-reveal-9-september-modena> (accessed on 8 March 2023).

19. Hua, J.; Zhou, L.; Gao, Q.; Feng, Z.; Wei, H. Influence of pre-chamber structure and injection parameters on engine performance and combustion characteristics in a turbulent jet ignition (TJI) engine. *Fuel* **2021**, *283*, 119236. [[CrossRef](#)]
20. Zhou, L.; Ding, Y.; Li, A.Q.; Song, Y.; Liu, Z.; Wei, H. Experimental study of gasoline engine with EGR dilution based on reactivity controlled turbulent jet ignition (RCTJI). *Fuel* **2023**, *331*, 125744. [[CrossRef](#)]
21. Atis, C.; Chowdhury, S.S.; Ayele, Y.; Stuecken, T.; Schock, H.; Voice, A.K. Ultra-lean and high EGR operation of dual mode, turbulent jet ignition (DM-TJI) engine with active pre-chamber scavenging. In *SAE Technical*; SAE International: Warrendale, PA, USA, 2020. [[CrossRef](#)]
22. Weißner, M.; Beger, F.; Schüttenhelm, M.; Tallu, G. Lean-burn CNG engine with ignition chamber: From the idea to a running engine. *Combust Engines* **2019**, *176*, 3–9. [[CrossRef](#)]
23. Bureshaid, K.I.; Feng, D.; Bunce, M.; Zhao, H. Experimental studies of gasoline auxiliary fueled turbulent jet igniter at different speeds in single cylinder engine. In *SAE Technical*; SAE International: Warrendale, PA, USA, 2019. [[CrossRef](#)]
24. Soltic, P.; Hilfiker, T. Efficiency and RAW emission benefits from hydrogen addition to methane in a prechamber-equipped engine. *Int. J. Hydrog. Energy* **2020**, *45*, 23638–23652. [[CrossRef](#)]
25. Dilber, V.; Sjerić, M.; Tomić, R.; Krajnović, J.; Ugrinić, S.; Kozarac, D. Optimization of pre-chamber geometry and operating parameters in a turbulent jet ignition engine. *Energies* **2022**, *15*, 4758. [[CrossRef](#)]
26. Benajes, J.; Novella, R.; Gomez-Soriano, J.; Martinez-Hernandez, P.J.; Libert, C.; Dabiri, M. Evaluation of the passive pre-chamber ignition concept for future high compression ratio turbocharged spark-ignition engines. *Appl. Energy* **2019**, *248*, 576–588. [[CrossRef](#)]
27. Bueschke, W.; Skowron, M.; Szwajca, F.; Wislocki, K. Flame propagation velocity in 2-stage gas combustion system applied in SI engine. *IOP Conf. Ser. Mater. Sci. Eng.* **2018**, *421*, 042009. [[CrossRef](#)]
28. Pielecha, I.; Bueschke, W.; Skowron, M.; Fiedkiewicz, Ł.; Szwajca, F.; Cieślak, W.; Wislocki, K. Prechamber optimal selection for a two stage turbulent jet ignition type combustion system in CNG-fuelled engine. *Combust Engines* **2019**, *176*, 16–26. [[CrossRef](#)]
29. Pielecha, I.; Wislocki, K.; Cieślak, W.; Fiedkiewicz, L. Prechamber selection for a two stage turbulent jet ignition of lean air-gas mixtures for better economy and emission. *E3S Web Conf.* **2018**, *70*, 03010. [[CrossRef](#)]
30. Divekar, P.; Han, X.; Zhang, X.; Zheng, M.; Tjong, J. Energy efficiency improvements and CO<sub>2</sub> emission reduction by CNG use in medium- and heavy-duty spark-ignition engines. *Energy* **2023**, *263*, 125769. [[CrossRef](#)]
31. Sahoo, S.; Srivastava, D.K. Effect of compression ratio on engine knock, performance, combustion and emission characteristics of a bi-fuel CNG engine. *Energy* **2021**, *233*, 121144. [[CrossRef](#)]
32. Jean, M.; Granier, P.; Leroy, T. Combustion stability control based on cylinder pressure for high efficiency gasoline engines. *Energies* **2022**, *15*, 2530. [[CrossRef](#)]
33. Heywood, J.B. *Internal Combustion Engine Fundamentals*; McGraw-Hill: New York, NY, USA, 1988.
34. Merkisz, J.; Pielecha, J.; Radzimirski, S. *New Trends in Emission Control in the European Union*; Springer Tracts on Transportation and Traffic; Springer International Publishing: Cham, Switzerland, 2014; Volume 4.

**Disclaimer/Publisher's Note:** The statements, opinions and data contained in all publications are solely those of the individual author(s) and contributor(s) and not of MDPI and/or the editor(s). MDPI and/or the editor(s) disclaim responsibility for any injury to people or property resulting from any ideas, methods, instructions or products referred to in the content.